

ISSN: 2692-5389

## Global Journal of Forensic Science & Medicine

DOI: 10.33552/GJFSM.2020.02.000532



**Research Article** 

Copyright © All rights are reserved by Goong Chen

# Computational Forensics for the Alleged Syrian Sarin Chemical Attack on April 4, 2017: What Actually Happened?

Goong Chen<sup>1,2,3\*</sup>, Cong Gu<sup>1</sup>, Theodore A Postol<sup>4</sup>, Alexey Sergeev<sup>1</sup>, Sanyang Liu<sup>5</sup>, Pengfei Yao<sup>6,7</sup> and Marlan O Scully<sup>2,8,9</sup>

\*Corresponding author: Goong Chen, Department of Mathematics, Texas A&M University, USA

Received Date: August 06, 2020

Published Date: November 09, 2020

#### **Abstract**

On April 4, 2017 a Syrian government air-attack at Khan Sheikhoun, Syria was followed by reports, photographs, and video data that indicated a significant number of casualties from exposure to toxic gases associated with the attack. This event was immediately followed by allegations that the deaths and injuries were caused by nerve agent released from a small crater produced by an air-dropped bomb on an asphalt covered road. The crater's size, shape, depth, contained debris, and surroundings were extensively documented in numerous videos and photographs, but until now, there has been no clear, science-based explanation of how the crater was formed. In this paper, we have applied advanced techniques from computational mathematics and mechanics to perform a forensic reconstruction of the crime scene. Based on 3D image analysis, we first show that the alleged site of the chemical attack had been tampered with, and essentially all of the public reports about the scene around the crater depend on observations made after the tampering had occurred.

Using mathematical modeling that utilizes the pertinent mechanics of fluids, solids, fracture and explosion based on LS-DYNA, our supercomputer simulation results have demonstrated the following:

- 1) We show that a bomb of cylindrical shape and high length-to-diameter (L/D) ratio that was attached to a metal tube arrived at a high speed and loft angle in excess of 200 m/s and 45° respectively and detonated at the surface of the asphalt road. The high L/D of the explosive charge and the attached metal tube indicates that the explosive charge was the warhead of a short-range rocket and the metal tube was the rocket's spent motor casing.
- 2) The cylindrical shape of the explosive charge, its loft angle, and its detonation at the asphalt surface completely explain the tear-shape (non-circular) of the crater rim and the location of deepest point in the crater which is at the round forward edge the tear-shaped crater-perimeter (the crater is not deepest at its middle). Our calculations also reveal in detail how the empty rocket motor casing was carried forward by momentum after the crater was produced by the much faster action of the explosion of the warhead. The calculations show how the forward-moving casing then gets buried in the crater's forward wall and bent at a large angle by a violent torque, similar to that produced when a pole vaulter converts forward



<sup>&</sup>lt;sup>1</sup>Department of Mathematics, Texas A&M University, USA

<sup>&</sup>lt;sup>2</sup>Institute for Quantum Science and Engineering, Texas A&M University, USA

<sup>3-5</sup> School of Mathematics and Statistics, Xidian University, Xian, China (on development leave from Texas A&M University)

<sup>&</sup>lt;sup>4</sup>Program on Science, Technology, and National Security Policy, Massachusetts Institute of Technology, Cambridge, USA

<sup>&</sup>lt;sup>6</sup>Key Laboratory of Systems and Control, Institute of Systems Science, Academy of Mathematics and Systems Science, The Chinese Academy of Sciences, China

<sup>&</sup>lt;sup>7</sup>School of Mathematical Sciences, University of Chinese Academy of Sciences, China

<sup>&</sup>lt;sup>8</sup>Department of Mechanical and Aerospace Engineering, Princeton University, USA

<sup>&</sup>lt;sup>9</sup>Baylor Research and Innovation Collaborative, Baylor University, USA

motion to torque by inserting the pole into the pivot. The bend in the motor casing from torque-producing pivoting action is sufficiently large to position the aft-end of the casing to well-beyond the forward edge of the crater's wall.

- 3) Crack and fissure patterns in the tubular metal casing are completely explained as produced by the high-pressure explosive gasses injected into the tube from the detonating rocket warhead. Our calculations therefore reproduce every significant observed physical feature of both the crater and the rocket motor casing.
- 4) Finally, we show that there was extensive tampering with the crater and debris, which led to misreporting by the press and social media based on non-expert analysis of photographs of the crater and debris after tampering had already occurred. The record of inaccurate reporting of this matter of international import by the press underscores the need for higher standards of scholarly and journalistic reporting and the use of real expert-science-based analysis before conclusions can be asserted.

In summary, the tear shaped rim of the crater is simply the result of a high L/D explosive charge of a rocket warhead and the bent and split metal tube found in the crater is no more than the spent motor casing of an indigenously manufactured short-range 122 mm artillery rocket. The observed and predicted orientation, bending and splitting of the rocket motor casing matches in every observed mechanical detail to the early-scene observations prior to the initiation of wide-ranging tampering with the evidence. The findings of this paper will help determine which parties should truly be held accountable for the brutal crimes and losses of life and injuries from this attack. By doing so, it will also strengthen the critical enforcement of international law and the noble objectives of the Chemical Weapons Convention.

#### Introduction

One of the largest U.S. military operations in 2017 occurred on April 7, when the Trump administration launched 59 Tomahawk cruise missiles from an Aegis Cruiser, the USS Porter, against the Syrian government's airbase at Shayrat, Syria. This attack was aimed at punishing the Syrian Government for an alleged sarin nerve agent attack that had taken place seventy-two hours earlier. The alleged attack took place on the morning of April 4, 2017 between 6 and 7 a.m. at Khan Sheikhoun (or, Khan Shaykhoun) in the Idlib Governorate of Syria. At the time the town was under the control of Tahrir al-Sham, previously known as the al-Qaeda affiliated al-Nusra Front. Press reports based on unconfirmed information obtained from these local occupying authorities claimed that more than 80 people were killed and 500-600 people were injured. Although it is clear that there was a Syrian government air-attack at Khan Sheikhoun on April 4, details of the actual events and consequences surrounding the occurrence remain in dispute. Allegations that the Syrian government attack included the intentional delivery of nerve agent were immediately reported by mainstream western media and by the United States, the major European powers, Turkey and the Gulf Cooperation Council. However, the Syrian and Russian Governments vehemently denied the unverified narratives collected from occupying Syrian rebels, and further claimed that no nerve agent was delivered in the attack. Russian anger about the US allegations against them was in part amplified because the flight plans for the attack had been routinely provided to the US Government in compliance with standing agreements.

If the Syrian Government (and also possibly its Russian ally) are the culprits responsible for the alleged nerve agent attack at Khan Sheikhoun, then it is an imperative of the Organization for the Prohibition of Chemical Weapons (OPCW) to expose these crimes. However, if the alleged attack did not take place, and the local rebel authorities misrepresented events to gain military and political advantage against the Syrian government, the UN and OPCW would

be responsible for a misapplication of the Chemical Weapons Convention that would undermine its most noble purpose - the discouragement and punishment of crimes against humanity. The objective of this paper is to provide the science-based evidence that will resolve this problematic international dispute and allow for the Chemical Weapons Convention to fulfill its intended purpose. The central piece of unambiguous physical evidence that is supposed to indicate that the alleged nerve agent attack occurred is a crater in the middle of an asphalt covered road in the northeast corner of Khan Sheikhoun. Both the White House intelligence report issued on April 11 and the OPCW report in June 2017 point to this crater as the source of the alleged sarin release. The assertions made in both reports are that a pipe within the crater was the vessel that was the source of the sarin release. The pipe was bent along its length and split open along a seam running parallel to its centerline. It has a diameter of 122 mm and a length of roughly 290 to 300 mm, which suggests it could have contained as much as 3.3 to 3.5 liters (6.5 to 7 kg) of sarin.

Since the alleged chemical attack occurred in a rebel-controlled zone, it was not accessible for inspection and evaluation by neutral parties (i.e., UN inspectors) due to the lack of guaranteed safe passage. Photographs of the crater provide the only available data for close examination by the Western World. Prior to the work presented in this paper, speculations on how the crater was formed have been limited solely to guesswork based on photographs and videos that reveal the crater's size, shape, depth, debris content, and its surroundings and location. These unresolved speculations about how the crater was formed have led to vigorous public debates, the resolution of which would determine whether or not a chemical attack had actually occurred. See Postol (the third author of this paper) [1] as one of the first to publicly press for a closer examination of this chemical attack and also to urge prudence in the assignment of guilt to Syria before the mechanism of how the

crater was formed could be definitively resolved. As far as other evidences related to the allegations of a nerve agent attack at Khan Sheikhoun are concerned, there are many unsettling pieces of evidence that raise serious questions about whether such an attack actually occurred. However, this paper addresses only the question of how the crater was formed. We show that computational forensics on this evidence alone settles the question of whether or not a nerve agent attack actually occurred at Khan Sheikhoun. Weapons analysts have studied the crater in order to understand what has happened. The following have been asserted (Case  $(H_1)$ ) or hypothesized (Cases  $(H_2)$ – $(H_3)$ ) as possibilities:

- 1) (H<sub>1</sub>) The broken pipe in the crater is the remnant of a sarin-containing chemical bomb dropped by a Syrian warplane.
- 2) (H<sub>2</sub>) In a report by the investigative reporter G. Porter [2], he described that an anonymous former U.S. senior intelligence officer examined the photos of the crater and indicated that its size is too small to be caused by a bomb. That analyst suggested that the crater looked like (or might be) just a pothole on the road. Pierre Spray, a former aeronautical engineer and a weapons analyst at the U.S. Department of Defense, reportedly reached a similar conclusion [2].
- 3) ( $\rm H_3$ ) In [1], Postol noticed that the broken pipe (from the bomb) has the shape that indicated the impact of a blunt crushing force from the top. Thus, he first theorized that the crater was caused by a bomb laid crossly upon a tube/pipe containing sarin and then detonated, releasing the chemical agent; see Figure 3.1(a).
- 4) (H<sub>4</sub>) Mikhail Ulyanov, a Russian Foreign Ministry disarmament expert, in a news report in New York Times [3], also indicated at U.N. that he believed the crater was caused by a bomb detonated on the ground (rather than air-dropped from an airplane belonging to the Syrian Government forces) and called into question how it could have been placed there. But he gave no further technical details. If Mr. Ulyanov was not himself a weapons analyst, then his assessment might well be attributed to be from some weapons experts in the Russian military.

The book of the criminal investigation on the Khan Sheikhoun chemical attack appeared to close after the OPCW issued its report [4] on June 29, 2017 and its ratification by the Joint Investigative Mechanism (JIM) on Syria in September. The report found that the Assad regime in Syria carried out the chemical attack. In [4], the OPCW concluded that sarin gas was used, and that it "likely" emanated from the crater. However, the Russian Government had been vociferously criticizing the OPCW and the JIM throughout the process because it viewed the OPCW investigation as having failed to follow basic investigative protocols that were established as part of the Chemical Weapons Convention. The Russians introduced a resolution in the UN Security Council on November 16 with

language that it argued would ensure that the investigation would continue, but with investigative protocols that it argued were less likely to lead to erroneous findings. When Russia's proposed tightening of investigative protocols was rejected, it vetoed the opposing American resolution to extend by one year the panel's mandate, which expired on November 16, 2017 [5]. There was no disagreement by any members of the Security Council, including Russia, that the cut off of the extension of the JIM was a tragic outcome stemming from disagreements about what constituted adequate and appropriate investigative protocols to be followed by the JIM.

Our objective in this paper is to perform a scientific forensic analysis. In forensic science, there are three important areas in investigating and assessing the various components of a "crime" scene:

- 1) Specific incident reconstruction
- 2) Event reconstruction and
- 3) Physical evidence reconstruction.

Our task here is mainly event reconstruction, i.e., item (2) above as we examine the connections between evidence and the physical sequence of events. Our work also has implications on the identities of those involved. Our study is basically a computerized reconstruction and reenactment. For example, in fire-arm related homicides, ballistic analysis is one of the most often used forensic tools. It can clarify inconsistencies between forensic analysis and the actual deeds of and evidence at the crime scene, and also point to more correct directions of subsequent investigations. Our study here is in principle no different from ballistic analysis, but the stakes of the outcome of the probe are high as it involves potential major international confrontations and the judicial assessment of the war crimes.

Nevertheless, reconstruction and/or reenactments of bomb detonation (as suggested by (H<sub>3</sub>) and (H<sub>4</sub>) above) are hard or impractical to perform, even at some reduced scales - bomb materials are hard to come by or to assemble by non-specialist academic researchers. It also requires proper funding for facility and time to set up and to make precise measurements. In particular, a detonation process is fast reacting, within the time scale of just a few tens of microseconds. This makes the measurements and observations all the more challenging. Under such circumstances, computational mathematics and mechanics may well be the investigative tool of choice, as it is naturally suited for analysis of numerous closely related scenarios. In this paper, we show, by using computational mathematics and mechanics, the forensics and ballistics that support the assessments that the chemical bomb was actually an improvised artillery rocket from a rocket launcher, and that the site of the crater was subject to tampering after it was initially formed. We have obtained the following results along the organization flow of the paper:

- i. Section 2: 3D image analysis by using 3D image reconstruction and the Eight-Point Algorithm [6] calculation shows that the crater site has been tampered with
- ii. Section 3: This is the core section of the paper. Here we show that detonation and impact simulations of a 122 mm rocket-propelled artillery unambiguously support that the cratering and projectile effects are consistent with the alleged scene of chemical attack, and the crack pattern in the expended rocket motor casing indicates manufacturing defects that mean that the rocket was most likely made locally. These are done by the computer-modeling software LS-DYNA
- iii. Section 4: Our simulations also dismiss and disprove the four hypothetical scenarios made by weapon analysts and others in  $(H_1)$ – $(H_4)$  above.

Concluding Remarks are given in Section 5. Concise technical details of the modeling and processing are deferred to Appendices I and II, especially the validation part. Our study on this problem started soon after the lead author read the article by Postol [1] in International Business Times on April 17, 2017. However, computer modeling, coding, supercomputing and visualization have proved to be totally challenging and slow-progressing, as each supercomputer run can easily take 3–5 days. Problems of such fast dynamics with detonation and destruction are well known to have high numerical instability and often tend to either diverge or produce physically inconsistent results. Fortunately, our prior experience [7] from the investigation of the rapid crash dynamics of the Germanwings Flight 9525, by incorporating the FEA (finite element analysis) and SPH (smooth particle hydrodynamics), has paved the foundation

for validation and then the eventual success of our computational work here, after more than half a year of devoted efforts. Important video animations are included with their URLs and are must-sees for the reader in order to understand the underlying dynamics.

### Tampering as Revealed by 3D Image Analysis of the Crater Site

#### Choosing the images

The goal here is to compare available images of the crater and to detect differences in the scenes of different pictures. We start from downloading four images from Postol's technical reports [1]. Using reverse image search engines Google and Tin Eye, we notice that each image is present in many online media sources in various versions that differ in image size and sharpness. For each image, we try to choose the best available copy which is typically ten times larger in the number of pixels than the original image. During this selection process, we can see many similar pictures of the crater, but taken from different angles. Finally, three additional images were chosen, that complement the original set of images. The images were divided in two groups:

- A. Without a red skeletal marker and
- B. Showing a rectangular red skeletal marker.

In the latter group, the images show some signs of advanced disintegration of the crater along its border, see the comparisons below. Therefore, we believe that the pictures in Group (B) were taken later than those in Group (A). The sources of the pictures and their sizes are listed in (Table 1).

Table 1: Sources and sizes of the crater images to be analy.	zed.
--	------

Image	Web address	Size (pixels)
A <sub>1</sub>	https://pbs.twimg.com/media/C8kEBpkXUAAXz1b.jpg	1200x800
$A_2$	https://www.dr.dk/images/other/2017/04/08/scanpix-20170405-090310-l.jpg	3500x2333
$A_3$	https://cdni.rt.com/russian/images/2017.08/original/59945338370f2ceb238b456e.jpg	1800x1000
$A_4$	https://pbs.twimg.com/media/C-0fQqJXYAAfJmr.jpg	1136x852
$B_1$	http://img.zeit.de/politik/ausland/2017-04/militaerschlag-syrien-donald-trump-giftgasanschlag-luftschlag-opposition-3/wide	1300x731
$\mathrm{B}_{2}$	https://i1.wp.com/rfsmediaoffice.com/en/wp-content/uploads/2017/04/4032.jpg?ssl=1	1920x1152
$B_3$	https://i.ytimg.com/vi/AqBqDzvtP-M/maxresdefault.jpg	1280x720

#### **Quick comparisons**

We noticed that the pictures  $(A_4)$  and  $(B_2)$  were apparently taken from similar points of view and at the same time of day. It allows us to compare them easily side-by-side; see (Figure 1.1). The comparison shows that the border of the crater expanded in  $(B_2)$  vs.  $(A_4)$  by cracking, collapsing of pavement and chipping of crack edges. This advanced deterioration of the pavement indicates that the picture  $(B_2)$  was taken at a later time. Considerable bending of the pipe on  $(B_2)$  vs.  $(A_4)$  as well as disappearance of loose debris on the pavement clearly shows tampering with the site. One can

already notice that the bending directions of the top of the pipe are different: one points outward of the crater in  $(A_4)$  while it points inward of the crater on  $(B_2)$ . But this visual inspection by the naked eye could be unreliable. Below, we quantify it by 3D image analysis that involves intricate geometric relations existing between 3D objects and their images.

#### Bent pipe as an evidence of tampering

The image analysis technique we have used can be found in Appendix I, where the important, so called fundamental matrix was calculated between images  $(A_1)/(B_1)$ , as well as between  $(A_1)/(B_2)$  and  $(A_1)/(B_3)$ . It allows us to show the epipolar lines in the image  $(A_1)$  that correspond to the location of the tip of the pipe in the images from Group (B). The intersection of epipolar lines shows the location of the tip of the pipe in the images from Group (B) as it would be seen in the image  $(A_1)$ . Figure 1.3 shows that the pipe has been bent in the images from Group (B) from outward to inward of the crater. In any law-enforcement investigation, it is

well understood that the initial crime scene must absolutely not be disturbed lest it should cause confusion or even distortion of the forensics. Here, our analysis clearly shows the effect of tampering by the local actors/parties/factions involved. The motivation is unclear. Indeed, in the next section, the subtle point of whether the top of the pipe should be pointing away from the crater or pointing inward to the crater can be answered from a "ballistic" study.





Figure 1.1: Comparison of the images  $(A_4)$  (left panel) and  $(B_2)$  (right panel). The observed differences in the crater shape are marked by yellow arrows. The orange arrow shows the bending direction of the pipe in image  $(B_2)$ . To make the comparison easier, we have made small perspective distortions of the image  $(A_4)$  (by approximately 10%) in order to make locations of four points (1–4) on the border of the crater exactly match in two images.

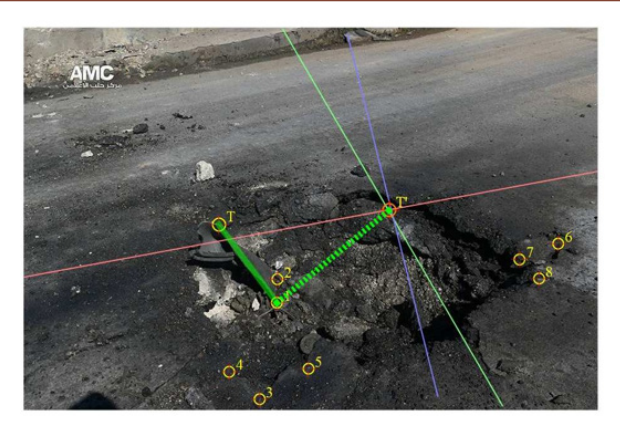








Figure 1.2: Eight corresponding points (1–8) in images (A<sub>1</sub>), (B<sub>2</sub>), (B<sub>2</sub>), (A<sub>3</sub>) and (B<sub>3</sub>). The point (T) marks the tip of the pipe.



**Figure 1.3:** The scene in image  $(A_1)$  with epipolar lines showing re-projection of the tip of the (T) from the images of Group (B) into the image  $(A_1)$ , red, green and blue lines for  $(B_1)$ ,  $(B_2)$ , and  $(B_3)$  images, respectively. Red circle at their intersection shows the tip from Group (B) as it would be seen in image  $(A_1)$ , as a point (T'). Bold green line connects points (1) and (T) and shows direction of the pipe in Group (A), while the dashed line does in Group (B).

## Computational Forensics on Cratering from Computer Modeling with LS-DYNA

Postol [1] first observed and assessed that the remnant pipe/ bomb in the crater looks like an improvised sarin dispenser made from a 122 mm artillery rocket. We hereby again closely examined the crater and the metal-bomb remnant and came to the same assessment that the broken pipe is the "carcass" of a 122 mm artillery rocket, after having dismissed several other scenarios (to be addressed shortly in this section, and discussed in detail in Section 4. Unfortunately, due to the lack of access to the physical site and objects, we cannot make any further confirmations about this. However, recall the Ghouta sarin attack in the suburb of Damascus in August 2013, where sarin dispensers were mounted on 122 mm artillery rockets as an improvised, effective chemical weapon (Figure 1.2). Any party can claim and blame that the other side(s) are repeating the earlier chemical attacks with the same modus operandi. We have also considered the possibilities of several other types of delivery projectiles, shapes/materials of sarin dispensers and the layout of explosives. Some of them will be discussed in Section 4. But those cases, after computationally simulated and then analyzed, have to be dismissed or disproved (Figure 1.3).

For the 122 mm artillery rocket, we first provide a description of their "fire power" in Figure 2.1. This particular variant of the 122 mm artillery rocket warhead weighs about 18.4 kg and has a 6.35 kg explosive charge. The exact weight of the charge in these easily purchased warheads varies somewhat but the explosive effects of charges of slightly different weights are essentially irrelevant to the findings shown in our calculations. Its trajectory properties are given in Graph 1. Their ballistic trajectory analysis including the rocket motor characteristics and their aerodynamic drag coefficients, after firing, is provided in Box 3.1, building on the prior work of Lloyd and Postol [8]. We are now in a position

to report our computational forensic findings based on the canonical, most versatile and recognized tool LS-DYNA [9], the chief commercialized product of computer modeling software made by the Livermore Software Corporation with more than fortyyears history of development. The technical details are provided in Appendix II. All the computations have been carried out on the ADA and Curie clusters at Texas A&M University's High-Performance Computing Center. Each run took about three days or longer. The major data for the rocket near landing and explosion is given in Table 2. We include Figure 2.2 with the sequence of six snapshots extracted from a video animation as the visualization output of our supercomputer results. The panels show the motion sequence, which leads to the end result of similarly what is observed in the photographs in the left column of Figure 1.2. The head (i.e., frontal portion) of the spent motor casing of the rocket is embedded in the soil near the edge of the crater (not at the center as some people have asserted or believed) and it is slightly bent forward and is pointing outward by the sudden torque that occurs when the warhead impacts and then becomes lodged under the asphalt surface. If we assume that the rocket casing was fabricated into a pipe by welding, our calculations show similarly the kind of split or fissure along a generatrix of the pipe. (A generatrix on a cylinder, here the pipe, is a line on the cylinder parallel to the axis of the cylinder).

**Table 2:** Parameters for the calculation of 122 mm rocket warhead upon impact on asphalt road.

Parameter	Value
Total weight of rocket	27 kg
Weight of TNT H.E.	8.1 kg
Weight of warhead metal	10.1 kg
Velocity	220 m/s
Angle	65°

#### **122 MM WARHEADS FAMILY**

#### HIGH EXPLOSIVE (H.E.)

Explosive war component for reactive ammunition cal. 122 mm

#### TECHNICAL CHARACTERISTICS

- component length - coupling thread for the fuse
- component body weight
- war component weight (charged)
- explosive component weight (TGAF-5) - detonator
- detonator weight
- operational temperatures range
- lethal range (lethal area)
- splinters number
- fuse equipping
- 605 mm Sp M 45x2 ~12,05 kg ~18,4 kg 6,35 kg AIX 1 -0,1 kg -40°C + +50°C
- min. 21,34 m (min.1430 sq.m)
- min. 2000 buc. MRV-U or MULTIFUNCTION fuze MFF-2T

#### H.E. with PREFORMED ELEMENTS

TOHAN PLANT HAS DEVELOPED THE 122mm WARHEAD WITH PREFORMED ELEMENTS THAT CAN REPLACE CLASSICAL HE WARHEAD

#### TECHNICAL CHARACTERISTICS

- mass of warhead 18.4 kg - mass of explosive charge (TGAF-5) 5.4 kg - number of preformed elements 12 pcs. - piercing thickness (steel sheet) at 7 m 20 mm

- lethal range (lethal area)

- fuze

min. 33 m (3420 sq.m)

MRV-U or MULTIFUNCTION fuze MFF-2T



Figure 2.1: 122 mm warheads family.

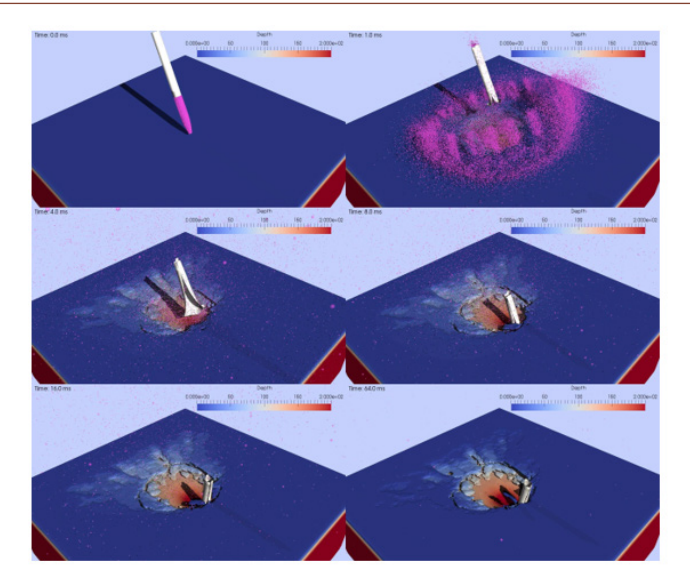


Figure 2.2: This simulation contains the key assessment of this article. Here we list panels of snapshots showing the impact and explosion of a 122 mm artillery rocket. The rocket casing has manufacturing defects, causing a linear crack on a generatrix. The crater has a rough radius of about 1.2 m and the remnant pipe has about 0.5 m above ground. For dynamic visualization, see the video in http://gucong.org/ blast/BlastSR2-J5A/.

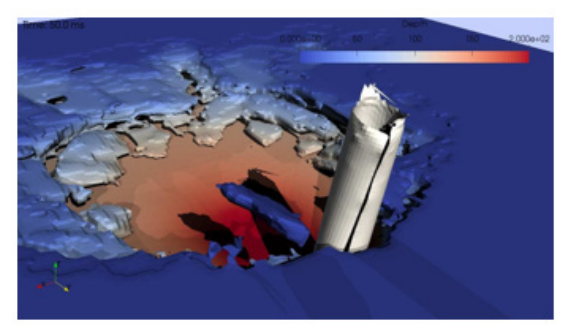
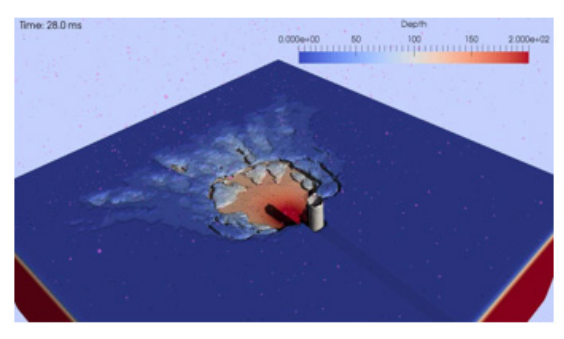


Figure 2.3: A zoomed-in view of the pipe in Figure 3.2.

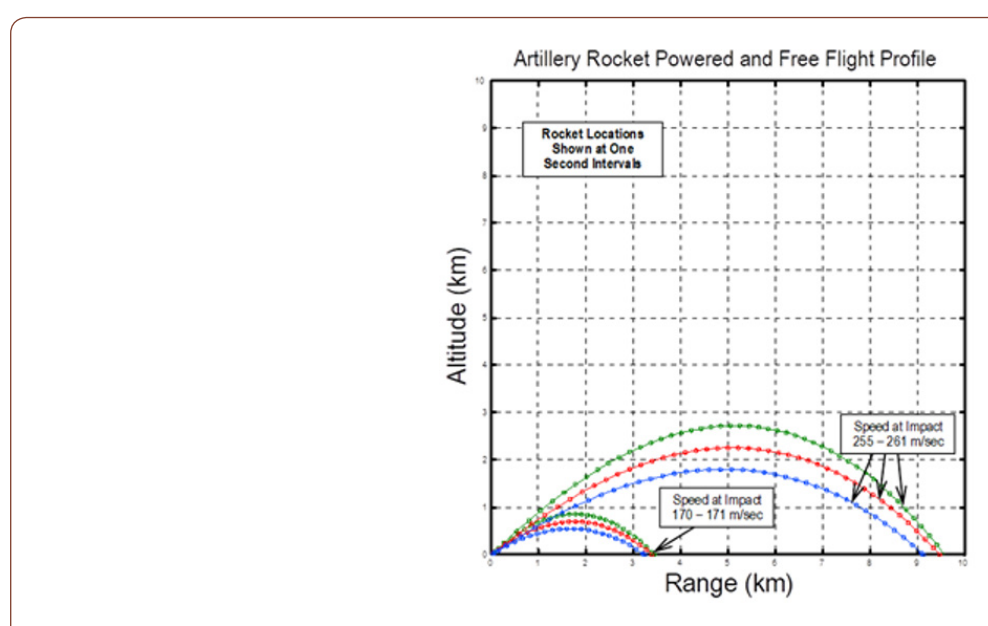


**Figure 2.4:** A snapshot of a 122 mm artillery rocket upon impact and explosion. This rocket is computed by using the same physical parameters as in Table 1, except that it does not have manufacturing defects. One sees no crack on the rocket casing. For dynamic visualization, see the video in http://gucong.org/blast/BlastSR2-J6A/.

#### Trajectory properties of a 122 mm artillery rocket

We assume that the rocket is traveling in two possible ranges: (i) 3.5-4 km; (ii) 10 km. From the following (Graph 1), for launch angles between  $35^\circ\text{-}45^\circ$ , the rocket will reenter at somewhat similar reentry angles. Rockets fired at ranges of 10 km or more have trajectories that are significantly modified by aerodynamic drag, which results in a larger reentry angle upon impact relative to the loft angle at the launch point. However, for a rocket fired at ranges

of order 5 km or less, aerodynamic drag does not play significant role to substantially increase the angle of the rocket at the impact point, nor does small changes in the loft angle significantly affect its range. Since the rocket motor casing (as seen in the photos of Section 2) is relatively small, we know that the rocket probably has a range of around 4–5 km. The angle at impact can have a range 45-70 degrees of variation. This range of variation will affect the crater's size and shape.

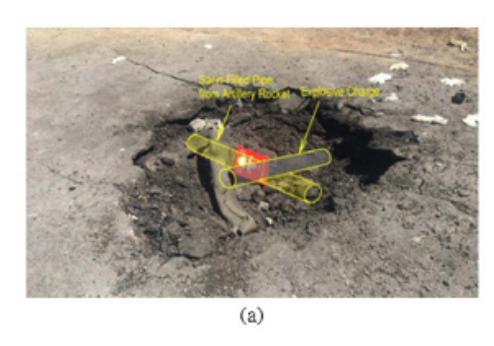


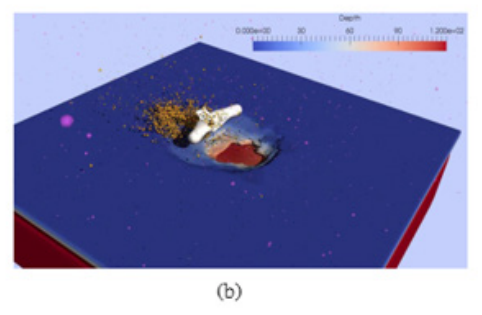
Graph 1: Trajectory properties of a 122 mm artillery rocket.

It is well known that cracks and fracture occur and propagate along the lines and locations where structural weakness and micro cracks preexist. The nearly linear crack split on the rocket motor casing (i.e., pipe) is due to the impact damage on the structure and then the propagation of the crack. The case computed in Figure 2.2 assumes the preexistence of structural weakness along a generatrix of the cylinder, due to possible welding in the fabrication of a pipe. The "line crack" can be seen in (Figure 2.3) as a zoomed-in view of the pipe in (Figure 2.2). We then have computed an additional case under exactly the same assumptions and with identical choices of parameters, but without any preexisting structural weakness on the pipe. The results show that the carcass then does not have a nearly linear crack; see Figure 2.4. This distinctiveness offers support that the rocket motor was manufactured more crudely with defects and thus, most likely locally. The propellant is thus probably filled with some fuel that was also locally produced. One such propellant that is commonly used in the manufacturing of improvised rocket motors is potassium nitrate (KNO<sub>2</sub>) and sugar. Thus, no room is reserved for sarin. The rest of the rocket can then be fabricated and assembled locally with a purchased warhead, igniter and nozzle to form an improvised rocket. The arrival azimuth is easily identified because the rocket is embedded at the forward edge/side of the crater and the bent spent rocket casing also points forward along the direction of arrival (that becomes pointing outward from the crater). The

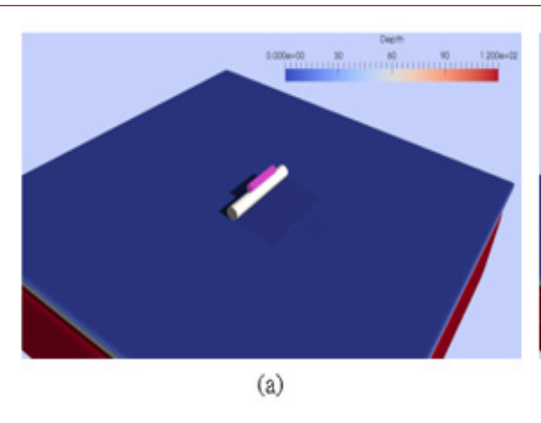
cracking of the asphalt surface surrounding the crater, clearly visible with a radiative pattern, is due to hot gases propagating through the underlying ground and pushing the asphalt vertically.

Remark 3.1. We need to bear in mind that even before the earliest photographs were taken of the crater as some were shown in the prior section, there might very well have been tampering with the (remnant) pipe therein. We also need to realize that our subsequent calculations do not necessarily capture possible inhomogeneities in the asphalt top, or more likely in the ground underneath. A soft spot in the ground below or a hard rock could significantly affect whether the pipe becomes lodged in the ground or simply bounces out of the crater, respectively. The computational mathematics and mechanics calculation essentially predict most or all of the observed fine features of the crater at Khan Sheikhoun. It is, therefore, unambiguous that the crater was created by a standard or more likely indigenously manufactured 122 mm explosive warhead of a type that is similar to what can be purchased in many parts of the world. There is no evidence of any sarin containing vessel. The split pipe that has been inaccurately identified as evidence of the container filled with sarin is simply the casing of the rocket motor that propelled the purchased warhead to the location of the explosion.





**Figure 3.1:** (a) A possible configuration first proposed by Postol [1] (b) A snapshot where one can see a totally different fracture pattern of the pipe. Thus, this configuration has been disproved. Video in <a href="http://gucong.org/blast/BlastSEC2/">http://gucong.org/blast/BlastSEC2/</a>.



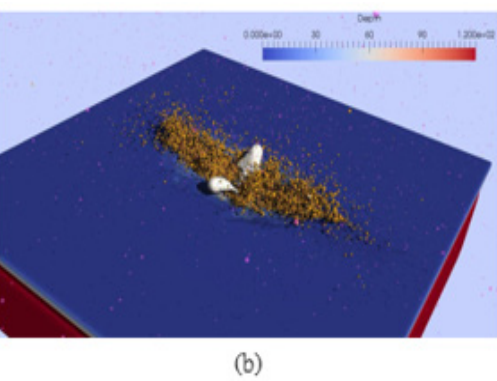


Figure 3.2: This layout between the explosive (on top) and the pipe is different from that in Figure 3.1. However, the fracture pattern of the pipe is similar, which is different from the pipe on the crater site so it is again dismissed. Video in <a href="http://gucong.org/blast/BlastSEC3/">http://gucong.org/blast/BlastSEC3/</a>.

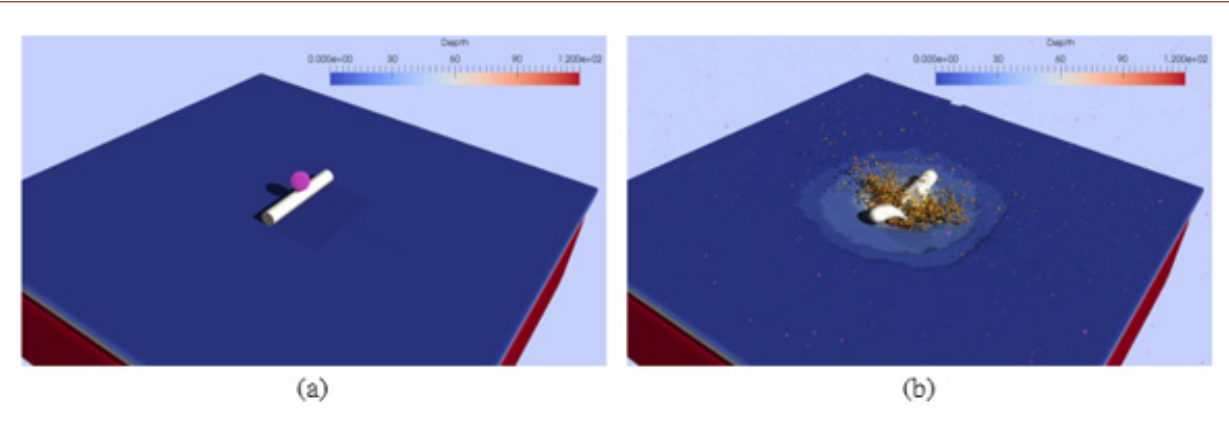


Figure 3.3: Here the explosive is spherical. Again, the eventual crack pattern in (b) leads to its dismissal. Video in <a href="http://gucong.org/blast/">http://gucong.org/blast/</a> BlastSEC4/.

#### Dismissals of Air-Dropped Bomb and Bomb-Detonation-on-the- Ground Scenarios

Four hypothetical possibilities have been described in  $(H_1)$ – $(H_4)$  in Section 1. Chronologically in our study, these were actually the scenarios investigated by us first as disproof's can be made rather quickly time wise. We now show that they do not agree with the evidence found on the crater site.

#### Dismissal of (H<sub>1</sub>)

Air-dropped bombs, due to its fins (or wings) guiding its vertical motion, invariably cause a radially symmetric crater with its largest depth at the center. It will not be possible for a bomb's remnant to get lodged near the rim and not near the center. So, this  $(H_1)$  can be easily dismissed.

#### Dismissal of (H<sub>2</sub>)

The crater is indeed a crater, not a pothole. A telling sign of an impact crater is the appearance of a radiative pattern of cracks emanating from the crater, which are clearly visible from the photos in Figure 1.1. Potholes may cause cracks, too. But those cracks are thermal and wear-and-tear cracks which lack a coherent pattern.

#### Dismissal of (H<sub>2</sub>) and (H<sub>4</sub>)

Postol [1] earlier suggested a blast configuration as shown in Figure 3.1. This configuration was the case first computed by us when we began this project. The outcome of the blast shows a totally different damaged and fractured pipe than the one seen in the crater, Figures 1.1 - 1.3. See also the associated video animation link in the caption of Figure 3.1. Setting up the pipe and high-explosive stick in different configurations, as given in Figures 3.2 & 3.3, only produces outcomes of a damaged and fractured pipe which look similar to that in Figure 3.1(b). Therefore, those hypothetical scenarios are also dismissed.

#### **Concluding Remarks**

Newsweek magazine [10] reported on Feb. 8, 2018 statements made by U.S. Secretary of Defense Mr. James Mattis that indicated

that "Now Mattis admits there was no evidence Assad used poison gas on his people". Such a lack of evidence (of the Syrian Government forces having used sarin) is hardly surprising, according to our investigation here. This paper demonstrated the use of a powerful new forensic tool based on computational mathematics and mechanics that allowed us to derive detailed information about the characteristics of an improvised munition that was used in a criminal attack on the civilian population of Khan Sheikhoun on the morning of April 4, 2017. We have shown that a crater that the Organization for the Prevention of Chemical Weapons (OPCW) found to be created by an air-dropped chemical weapon was instead created by an improvised short-range artillery rocket armed with a small explosive warhead. The conclusions of this analysis are unambiguous: the OPCW incorrectly identified this crater as the source of a chemical release by an air-dropped bomb - the crater is instead from the impact and explosion of a short-range improvised artillery rocket. This fact, when combined with other observations (not included in this study), also indicates that the crater contained no observed evidence of a sarin container. The bent pipe that was misidentified by the OPCW as a container is instead the casing of a spent rocket motor. The rocket motor casing was bent by an intense impulsive torque as the rocket's warhead stopped suddenly as it penetrated the ground and detonated. The observed and demonstrated "teardrop" shape of the crater rim was due to the geometrical spreading of the detonating explosive gases from the extended length and the roughly 45° angle to the ground of the explosive charge in the warhead. And, the cracks in the asphalt surface around the crater were caused by the hot gases of the exploding warhead spreading through the ground and pushing the asphalt upward.

We fully support policies that aim to hold accountable the perpetrators of horrifying war crimes like chemical attacks and other acts of terrorism. In the current case of the alleged sarin attack at Khan Sheikhoun, our study has unambiguously ruled out that the centerpiece bomb crater was caused by an air-dropped bomb from a Syrian warplane. The implications of this finding do not necessarily

mean that there are no parties to be held accountable for the brutal injuries and losses of life at Khan Sheikhoun, but it does show that the findings of both the White House and OPCW reports on this matter are wrong. What this means in turn, is that the story is much more complicated than what has been claimed. The implications for the future is that by performing computational forensics as in this paper, international organizations and governments can gain much deeper insights about events that may have been preventable or that require the assignment of attribution so as to hold the appropriate individuals and organizations accountable.

The Chemical Weapons Convention can have no meaning if its enforcement is not based on solid science-based forensics. The findings of this analysis demonstrate the key role that sciencebased forensics can play in the analysis of criminal events that are of international significance. Without these tools, it is simply not possible to reliably determine attribution for criminal events, and if attribution cannot be reliably determined, the Chemical Weapons Convention will not be enforceable, and it will lose its meaning. We hope that the science-based contributions reported in this paper will strengthen the critical enforcement and nobility of the Chemical Weapons Convention. Our work emphasizes the physical and computational nature of Computational Forensics and tries to stay clear of the human factors. However, an even more worrisome. unspoken finding by us is that Syrian rebels and Islamic radical elements were alleging chemical attacks to heighten confrontations between Russia and the West operating in the Syrian theater. Those parties are clever to sense the antagonism between the East and West and want to exploit it to their advantages by way of allegations of chemical attacks. The West must be made fully aware of such a

## Appendix I: Corresponding Points, Epipolar Geometry and the Fundamental Matrix

This Appendix I offers a brief technical background for images analysis in Section 2. From a mathematical point of view, an image is a projective mapping of a three-dimensional object into a plane. Since two different images of the same object may be results of different projections, their comparison is not straightforward. However, locations of a given physical point in two different images are closely related. Introducing homogeneous coordinates  $\mathbf{x} \equiv (x, y, 1)$ , as in projective geometry, of a point (x, y) in the first image and  $\mathbf{x}^I \equiv (\mathbf{x}^I, \mathbf{y}^I, \mathbf{1})$  of the corresponding point  $(\mathbf{x}^I, \mathbf{y}^I)$  in the second image, this relationship can be expressed as the linear constraint [11, 12].

$$x'^{\mathrm{T}}Fx = 0 \tag{1}$$

The matrix F in (1) is called the fundamental matrix. It depends only on internal parameters of the cameras and their positions. If the location of a point in the second image, xJ, is known, then possible locations of the same point in the first image, x, may be anywhere on the line defined by (1). This line is known as epipolar line. Our first task is calculating the fundamental matrix between two images using a set of eight pairs of corresponding points. We write down a set of eight homogeneous equations

$$\boldsymbol{x}^{\prime(n)^T} F \boldsymbol{x}^{(n)} = 0 \tag{2}$$

for each pair of corresponding points  $(x^{l(n)}, x^{(n)})$ ,  $n = 1, \dots 8$ . Since F is  $3 \times 3$  matrix with 8 unknown elements (we could always set  $F_{11} = 1$  because of homogeneity of the equations), 8 equations are generally sufficient to resolve the linear system for 8 unknowns. The corresponding points of the images were selected manually as some prominent "landmark" points that are clearly visible in each photo and that are associated with solid and unmovable physical objects. Our choice of corresponding points is shown in Figure 1.2.

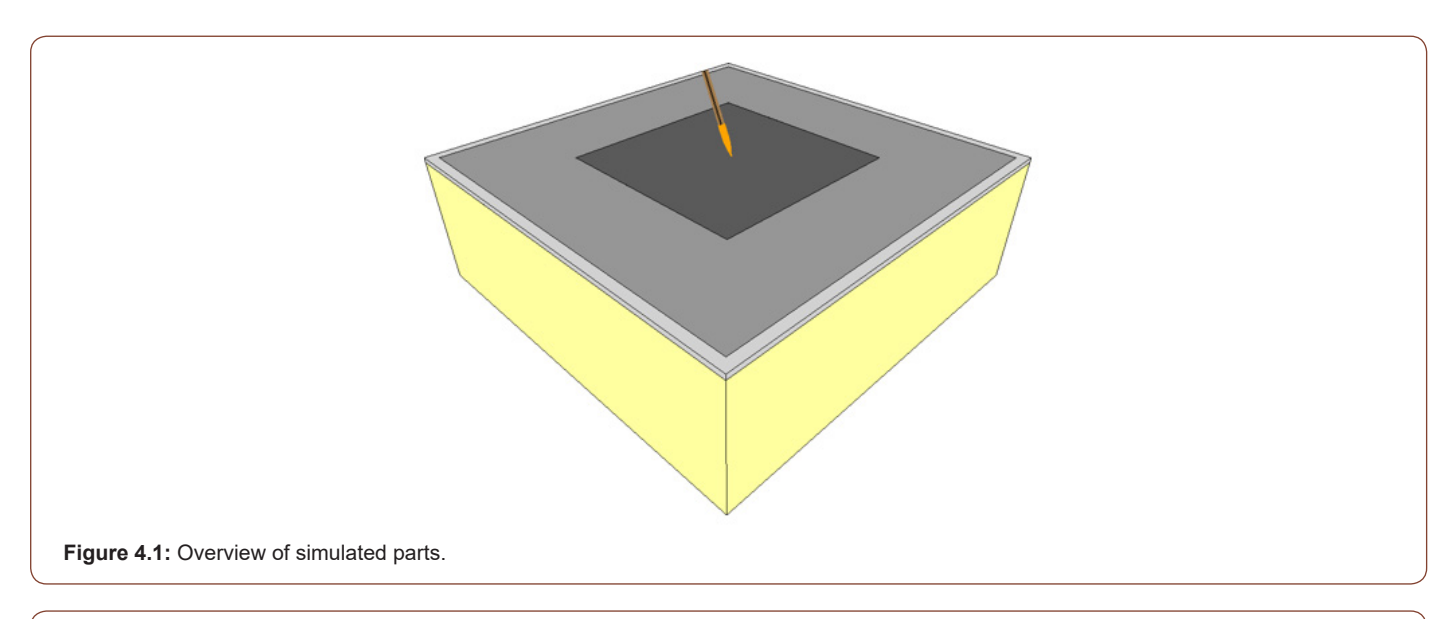
## Appendix II: LS-DYNA Computer Modeling of Explosion and Impact; Validation

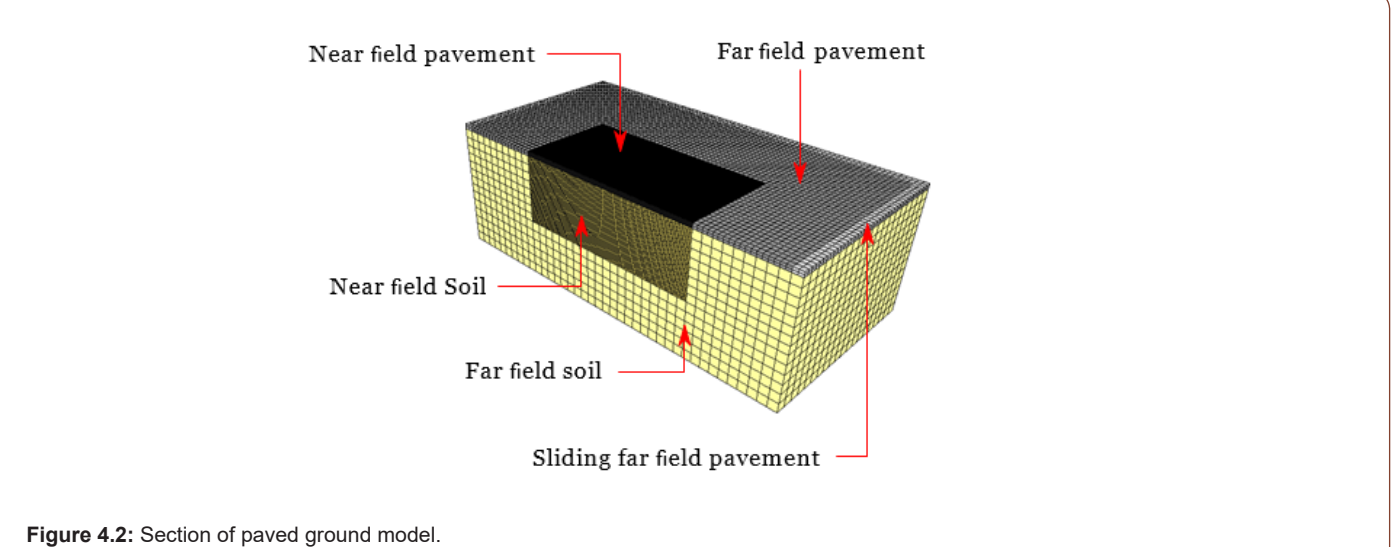
Modeling and computation of the problem under consideration require fundamental mathematical models like partial differential equations for aerodynamics (hot gas), solid dynamics (paved road), fracture mechanics, explosion dynamics, and their interactions. By proper set-up, LS-DYNA is able to take all of them into account. This Appendix provides the foundation for modeling and computation methodologies for Section 3. LS-DYNA is a general-purpose finite element analysis software developed by LSTC [9]. It has accumulated amazingly numerous capabilities and functions that are powerful in simulating complex real-world transient dynamic problems such as crash and explosion. The authors have successfully used LS-DYNA to study the pulverizing crash of Germanwings Flight 9525 [7], where it is found that a combination of Finite Element Analysis (FEA) and Smoothed Particle Hydrodynamics (SPH) can yield excellent results.

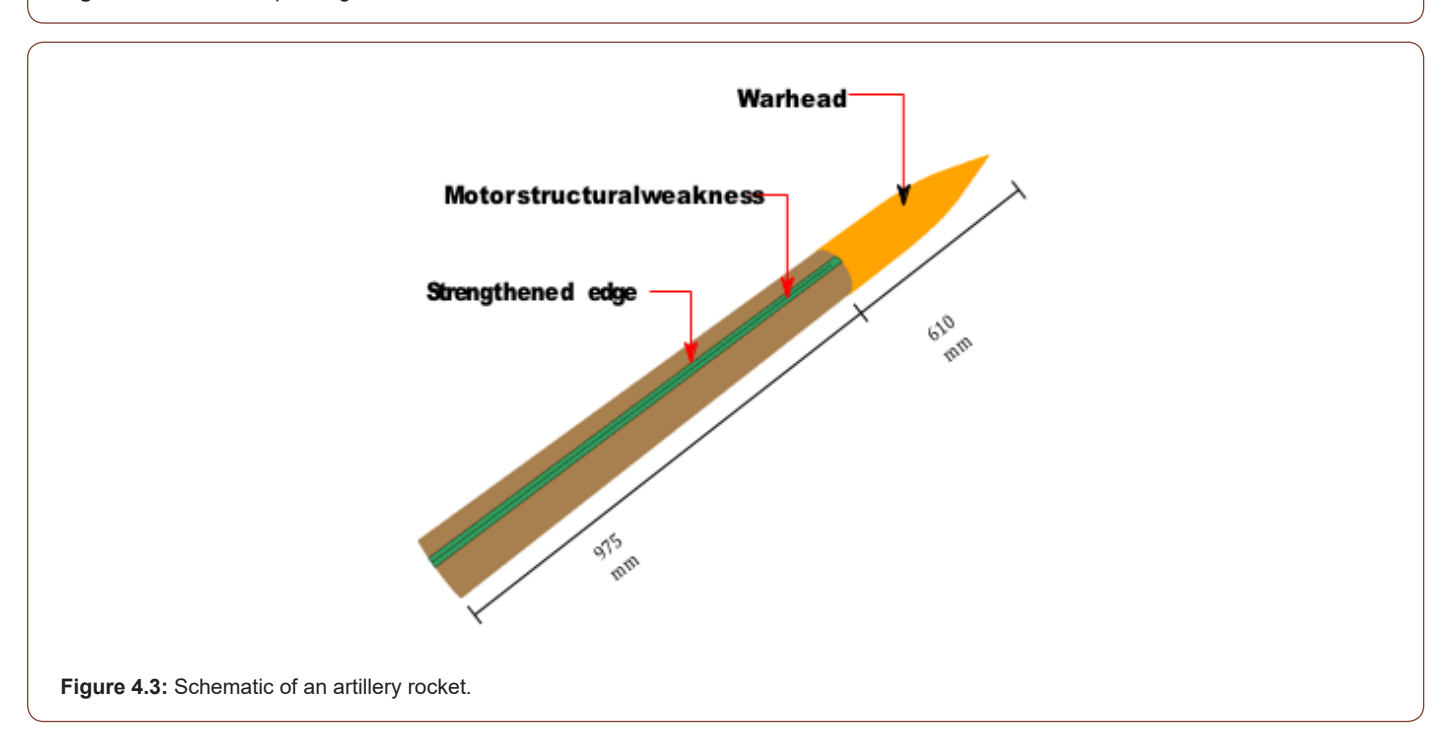
The problem of asphalt pavement under blast and impact load has been studied numerically using LS-DYNA by other researchers; see [13], for example. In the current study, we use solid elements to model the paved road, shell elements to model the structure of the artillery rocket, and SPH particles to model the warhead including the high explosives. The process of the explosion and impact of the artillery rocket, consisting of a warhead and a motor pipe behind, can be described as follows. The warhead explodes upon contact with the road, creating damages. The motor part then keeps moving downward and crashes into the ground. The basic spatial setup of the simulation is shown in (Figure 4.1). Details of the modeling of each component are discussed below.

#### Modeling of paved road

The road is modeled as an asphalt pavement of 10 cm in thickness, and a soil foundation underneath. The pavement consists of three parts, the near field, the far field (coarse grids) and the sliding far field. The sliding far field is tied to the soil underneath, but its tangential sliding is permitted. The soil is also modeled with a near field part and a far field part with a different grid size. See Figure 4.2 for a cross-section of the ground. The material model for the asphalt chosen in LS-DYNA is MAT\_CONCRETE\_DAMAGE\_REL3 with parameter generation, while the material model for the soil is MAT\_SOIL\_AND\_FOAM. Major material parameters are shown in Table 3.







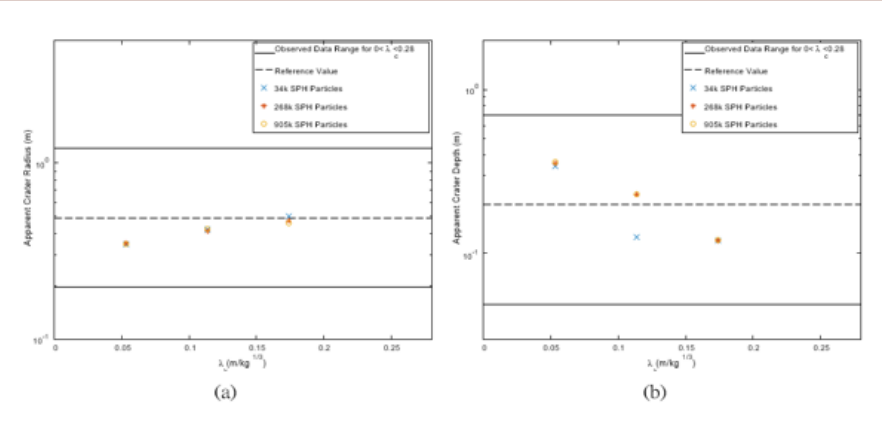


**Figure 4.4:** Ball-shaped, 5 lb TNT charge detonated at various locations above the soil. Comparison of (a) apparent crater radius and (b) apparent crater depth, with [15].

#### Modeling an artillery rocket

The artillery rocket consists of a warhead and a motor. The warhead has a metal casing with high explosives inside They are both modeled with SPH. The motor pipe has a longitudinal structural weakness intended to signify a welding seam and is modeled by collocated nodes tied with CONSTRAINED\_TIE-BREAK. There is a strengthened edge (larger thickness) along the seam of the structural weakness. See Figure 4.3. The material model of high explosive is MAT\_HIGH\_EXPLOSIVE\_BURN. The important equation of state of high explosives is EOS\_JWL (the empirical Jones-Wilkins-Lee equation of state), given by

$$p = A \left( 1 - \frac{\omega}{R_1 V} \right) e^{-R_1 V} + B \left( 1 - \frac{\omega}{R_2 V} \right) e^{-R_2 V} + \frac{\omega E}{V}$$

The material model for steel is MAT\_PLASTIC\_KINEMATIC, whose strain rate effect is accounted for by the Cowper-Symonds model

$$\frac{\sigma_{y}}{\sigma_{0}} = 1 + \left(\frac{\epsilon}{\varepsilon}\right)^{1/p}$$

#### **Contact modeling**

Contact settings are summarized in (Table 6). Erosion is enabled for the pavement to simulate damage and perforation. The

motor pipe has a "tie on contact" type of contact with the soil, which is meant to simulate the fixation of the motor pipe in the ground after having lodged into the soil. Static frictional coefficient is set to be 0.8 and dynamic frictional coefficient is set to be 0.6 where applicable.

#### Validation of SPH blast simulation

Validation is a crucial, indispensable part of any computational mechanics study. The computed data must be validated against those from experiments. Artillery rocket explosion damage data are hard (or, nearly impossible) to come by. Therefore, we have done the next best thing: validating (Tables 4,5,6) our explosion data versus the crater formation data from high-explosive blasts collected by the U.S. Army Corps of Engineers [14,15]. In this validation, we use Smoothed Particle Hydrodynamics (SPH) to simulate buried, contact (0 <  $\lambda_c$  < 0.053), and near field (0.053 <  $\lambda_c$  < 0.4) blast load, where  $\lambda_c$  is the reduced charge position with unit m/kg1/3. In our situation,  $\lambda_{c} \approx 0.12$  if the warhead is detonated upon ground impact with a 45° landing angle. In our validation simulation, we set up a ball-shaped 5 lb TNT charge at various locations above the soil. The shear modulus of soil is lowered to 20 MPa, from 60 MPa in Table 3, which is meant to model a stronger gravel rich mixture. In Figures 4.4(a) & (b), craters in our simulation are compared with the cratering data collected by the U.S. Army Corps of Engineers [15]. The data manifest that they lie well within the range of experiments.

Table 3: Material parameters for the paved road.

Parameter	Value
Density of asphalt	2320 kg/m3
Unconfined compression strength of asphalt	4.6 Mpa
Strain rate effect for asphalt	[13, Figure 6]
Maximum principal strain at erosion for asphalt	0.08
Minimum principal strain at erosion for asphalt	-0.08

Density of soil	2100 kg/m³
Shear modulus of soil	60 MPa
Yield coefficients of soil	[14, Table 2]
Compressibility of soil	[14, Figure 14]

Table 4: Parameters for high explosive (TNT).

Parameter	Value
Density	1630 kg/m3
Detonation velocity	6930 m/s
Chapman-Jouget pressure	21 GPa
A in JWL	371.2 GPa
B in JWL	2.23 GPa
R <sub>1</sub> in JWL	4.15
$R_2$ in JWL	0.95
ω in JWL	0.3
Initial E in JWL	7 GJ/m3
Initial V in JWL	1

Table 5: Parameters for rocket steel parts.

Parameter	Value
Density of Steel	7800 kg/m3
Young's modulus	200 GPa
Poisson's ratio	0.29
Yield stress	310 MPa
Tangent modulus	1 Gpa
Kinematic hardening parameter	0.3
C in Cowper-Symonds model	40 s-1
p in Cowper-Symonds model	5
Effective plastic strain at erosion	0.7
Motor thickness	3 mm
Motor edge thickness	5 mm
Warhead casing thickness	6 mm

Table 6: Contact settings.

Slave	Master	Contact
Warhead	Pavement	ERODING_NODES_TO_SURFACE
Warhead	Other	AUTOMATIC_NODES_TO_SURFACE
Motor	Pavement	ERODING_SURFACE_TO_SURFACE
Motor	Soil	AUTOMATIC_SURFACE_TO_SURFACE_TIEBREAK (Option 1 - tie on contact)
Sliding far field pavement	Soil	AUTOMATIC_SURFACE_TO_SURFACE_TIEBREAK (Option 4 - slide)
Near field pavement	Far field pavement	TIED_NODES_TO_SURFACE
Near field soil	Far field soil	TIED_NODES_TO_SURFACE
Other	-	AUTOMATIC_SINGLE_SURFACE

#### Acknowledgement

S. Liu is partially supported by The National Natural Science Foundation of China Grant No. 61373174. P. Yao is partially supported by The National Natural Science Foundation of China Grants No. 61473126 and No. 61573342, and Key Research Program of Frontier Sciences, CAS, No. QYZDJ-SSW-SYS011. M.O. Scully is partially supported by The Robert A. Welch Foundation Grant No. A-1261. We thank Texas A&M University's High-Performance Computing Center for the generous allocation of supercomputing hours on the Ada and Curie clusters.

#### Conflict of Interest

No conflict of interest.

#### References

- TA Postol (2017) A Quick Turnaround Assessment of the White House Intelligence Report Issued on April 11,2017 About the Nerve Agent Attack in Khan Shaykhun, Syria. URL: https://d.ibtimes.co.uk/en/file/99/postol-report-1.pdf (visited on 11/02/2017).
- G Porter (2017) Have We Been Deceived Over Syrian Sarin Attack? Scrutinizing the Evidence in an Incident Trump Used to Justify Bombing Syria. URL: https://www.alternet.org/grayzone-project/what-really-happened-khan-sheikhoun (visited on 11/02/2017).
- R Gladstone (2017) Russia U.S. Diplomatic Dispute Could Endanger Syria Investigation. URL: https://www.nytimes.com/2017/10/20/ world/middleeast/syria-russia-chemicalweapons. Html (visited on 11/02/2017).
- (2017) Technical Secretariat. Report of the OPCW Fact-Finding Mission in Syria regarding an alleged incident in Khan Shaykhun, Syrian Arab Republic. URL: https://www.opcw.org/fileadmin/OPCW/Fact\_Finding\_ Mission/s-1510-2017\_e\_.pdf (visited on 11/02/2017).

- (2017) Security Council Meetings Coverage. Security Council Fails to Adopt 2 Draft Resolutions on Extending Mandate of Joint Mechanism Investigating Chemical Weapons Attacks in Syria. URL: https://www. un.org/press/en/2017/sc13072.doc.htm (visited on 01/08/2018).
- 6. HC Longuet Higgins (1981) A computer algorithm for reconstructing a scene from two projections. Nature 293: 133-135.
- G Chen, YC Wang, A Perronnet, C Gu, P Yao, et al. (2017) The advanced role of computational mechanics and visualization in science and technology: analysis of the Germanwings Flight 9525 crash. Physica Scripta 92(3): 033002.
- R Lloyd, TA Postol (2014) Possible Implications of Faulty US Technical Intelligence in the Damascus Nerve Agent Attack of August 21, 2013.
  URL: https://www.voltairenet.org/IMG/pdf/possible-implications-of-bad-intelligence.pdf (visited on 11/02/2017).
- LS-DYNA. Livermore Software Technology Company. URL: http://www. lstc.com/products/ ls-dyna.
- Newsweek article: US Government has No Evidence on April 2017 Khan Sheikhoun Attack. URL: http://www.newsweek.com/now-mattisadmits-there-was-no-evidence-assad-using-poison-gas-his-people-80 201542
- Y Ma, S Soatto, J Kosecka, SS Sastry (2012) An Invitation to 3-D Vision: From Images to Geometric Models. Springer Science & Business Media.
- 12. R Hartley, A Zisserman (2003) Multiple View Geometry in Computer Vision. Cambridge university press, UK.
- 13. J Wu, L Li, X Du, X Liu (2017) Numerical study on the asphalt concrete structure for blast and impact load using the Karagozian and case concrete model. Applied Sciences 7: 202.
- EL Fasanella, KH Lyle, KE Jackson (2009) Developing soil models for dynamic impact simulations. URL: https://ntrs.nasa.gov/search. jsp?R=20090022374.
- J Strange, C Denzel, T McLane III (1961) Cratering from High Explosive Charges. Analysis of Crater Data. Tech. rep. Army Engineer Waterways Experiment Station, Vicksburg, USA.